

procedure used in [3] naturally yields functions of non-substitutive kind, in the sense that these functions reduce to the standard (regular) zeroth-order basis functions in the limit for singularity coefficient $\nu = 1$. In all applications the singularity coefficient ν must be known a priori [1, 3]; for a perfectly conducting wedge of internal wedge angle α , one has $\nu = \pi/(2\pi - \alpha)$. The smallest value, $\nu = 1/2$, occurs for a half plane ($\alpha = 0$), while $\nu = 1$ represents an infinite flat plane.

The bases derived in [3] are not satisfactory because: a) in the neighborhood of an edge the bases should be of additive kind (see [1, 4]); b) the vector component normal to the edge-profile of the edge-singular functions ${}^e\mathbf{\Lambda}_i(\mathbf{r})$ does not vanish as ξ^ν , ξ being the parent variable vanishing on the edge profile. The *edgeless function* for the edge-singular triangular element given in [1] is also not satisfactory, since its divergence does not properly model the charge density distribution. There also exist dependencies that have not been pointed out in [1] for the higher order singular triangular bases given in there. We have found a new technique to derive singular bases of the lowest order. These bases can be obtained by use of scalar generating functions defined on a given (triangular or quadrilateral) element. The singular bases derived in this manner properly satisfy all the requirements (conformity, completeness, additive nature, proper modelling of both the current and charge distributions, etc.).

Figure 3 shows the behavior of some of the new triangular vector functions. The corner nodes of the triangle are locally numbered from 1 to 3, and each edge of the triangle is given the same local-order number already associated with its opposite corner. This figure has been obtained by assuming edge 3 of the triangular element (the edge opposite to node 3) to be singular. The first vector plot is relative to the *regular* divergence-conforming function $\mathbf{\Lambda}_1(\mathbf{r})$, that has a vanishing normal component along edge 2 and 3, with a constant normal component along the first edge (opposite to node 1). The second row of Fig. 3 shows the behavior of the edge-less function ${}^e\mathbf{V}_3(\mathbf{r})$, that has a vanishing normal component along all the three edges of the element, but with a normal component that, toward the third edge, goes to zero as ρ^ν , ρ being the distance from the edge profile lying on edge 3. The divergence of ${}^e\mathbf{V}_3(\mathbf{r})$ is reported on the right-hand side of the figure. This divergence is singular as $\rho^{\nu-1}$ in the neighborhood of the third edge, so that this function is able to model the edge singularity of the charge density distribution on the triangular element. The last row at bottom of Fig. 3 represents the behavior of the *singular* divergence-conforming

function ${}^e\mathbf{\Lambda}_1(\mathbf{r})$, with a vanishing normal component along edge 2 and 3, and with a singular normal component along the first edge (opposite to node 1). This function, together with the ${}^e\mathbf{\Lambda}$ function associated with the second edge (that is ${}^e\mathbf{\Lambda}_2(\mathbf{r})$), is able to model the $\rho^{\nu-1}$ singularity of the current component parallel to the edge profile (which in this case happens to be normal to the first edge). Obviously, the vector plot relative to this latter function has been obtained by omitting all the samples on the third edge of the triangle, because of the infinite value of this function on the singular edge. The divergence of ${}^e\mathbf{\Lambda}_1(\mathbf{r})$ is reported on the right-hand side, at bottom of the figure. Once again, this divergence is singular as $\rho^{\nu-1}$ in the neighborhood of the third edge, so that also this function is able to model the edge singularity of the charge density distribution on the triangular element.

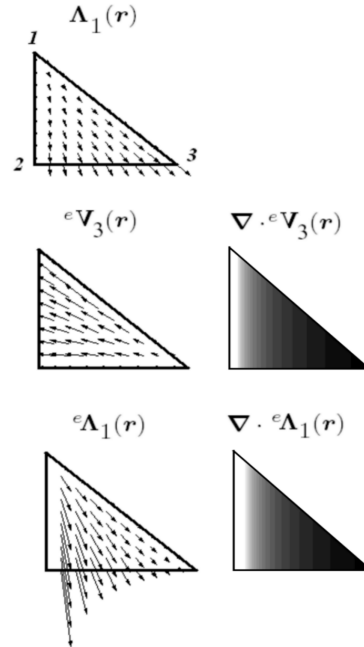


Figure 3: Regular (top) and edge-singular (mid-bottom) triangular vector functions: the 3rd edge (opposite to node 3) is assumed to be singular.

3 INTEGRATION OF THE SINGULAR BASES IN MoM APPLICATIONS

The main problem in MoM applications that use the Galerkin method is the evaluation of the MoM integrals for self and near-self elements. The difficulty of this problem is worsened when singular bases are in use. At the Conference we will report some of the techniques we have developed and used to solve this problem. As a matter of fact,

we still consider the integration problem as open when dealing with singular expansion and/or testing functions. We attached the integration problem in several different ways, by studying in detail the results provided by each integration method we have tested. For example, Fig. 4 shows the intensity of the field over a triangular *test-element* (reported at left) due to the edge-singular *source-element* shown at right. These are triangular near-self elements with the hypotenuse in common. The color scale used to report the intensity shows higher values with light grey color.

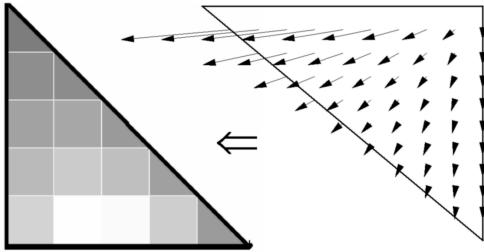


Figure 4: Near-self elements with a common hypotenuse: field intensity over the triangular *test-element* (reported at left) due to the edge-singular *source-element* shown at right.

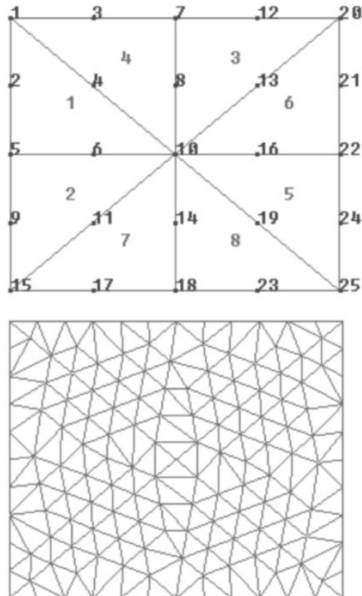


Figure 5: Rectangular plate problem: 8 (top) and 256 (bottom) triangular elements are used to mesh the structure.

4 NUMERICAL RESULTS

The test problem considered in this section is the problem of a rectangular plate ($0.5\lambda \times 0.6\lambda$) normally illuminated by a plane wave. The EFIE of this problem was numerically solved by use of the meshes shown in Fig. 5. We studied this problem by use of regular as well as singular bases defined over the coarse and the dense mesh. The results reported in Fig. 6 show the magnitude of the far-field scattered by the plate versus the observation angle ϕ ($\phi = 0$ at backscattering).

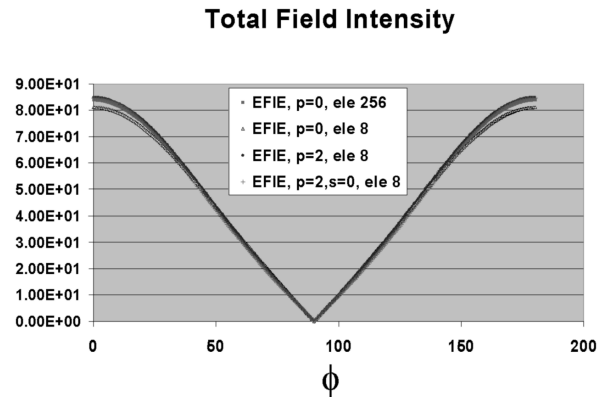


Figure 6: Magnitude of the far-field scattered by a rectangular plate ($0.5\lambda \times 0.6\lambda$) normally illuminated by a plane wave. Results are reported versus the observation angle ϕ , with $\phi = 0$ at backscattering.

To appreciate the differences in the obtained numerical results we report in Fig. 7 the results in the region $0 \leq \phi \leq 25^\circ$. This figure shows that the results obtained by working with the coarse mesh (8 elements) and with regular zeroth-order (i.e., $p = 0$) bases are rather poor. To improve the quality of the results, without using singular bases, one can either use regular ($p = 0$)-order elements on a denser mesh (256 elements), or still work on the coarse mesh but with higher-order (for example $p = 2$) regular elements. The results obtained by working on the coarse mesh (8 triangles) with singular ($s = 0$) elements of regular order $p = 2$ are in good agreement with those provided by use of regular elements of order $p = 2$ on the denser mesh.

These results show that singular high-order divergence-conforming bases should provide more accurate and efficient numerical solutions of surface integral problems.

5 CONCLUSIONS

This paper presents new singular divergence-conforming vector bases that incorporate the edge

Total Field Intensity

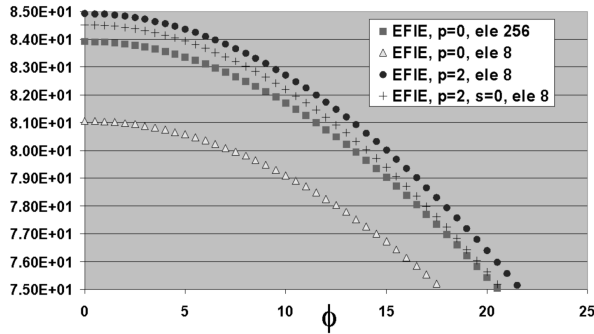


Figure 7: Magnitude of the far-field scattered by a rectangular plate ($0.5\lambda \times 0.6\lambda$) normally illuminated by a plane wave. Results are reported versus the observation angle ϕ , with $\phi = 0$ at backscattering.

conditions on curved triangular elements. Higher order bases can be obtained from these new bases by application of the technique already reported in [1]. Our bases are fully compatible with the standard, high-order regular vector bases used in adjacent elements. These singular bases guarantee normal continuity along the edges of the elements allowing for the discontinuity of tangential components, adequate modelling of the divergence, and removal of spurious solutions. Sample numerical results confirm the faster convergence of these bases on wedge problems.

Acknowledgments

This work was supported by the Italian Ministry of Education, University and Research (MIUR) under the FIRB grant RBAU01M9PF: *Vector expansion functions for singular fields*.

References

- [1] R. D. Graglia, and G. Lombardi, "Singular higher order complete vector bases for finite methods," *IEEE Trans. Antennas Propagat.*, vol. 52, no. 7, pp. 1672-1685, July 2004.
- [2] R.D. Graglia, G. Lombardi, and D.R. Wilton, "Singular Higher Order Models of Surface Integral Problems," *Proc. IEEE AP-S Int. Symp. and URSI Nat. Radio Sci. Meeting*, Monterey, California, USA, vol. URSI, p. 281, June 2004.
- [3] W.J. Brown and D.R. Wilton, "Singular basis functions and curvilinear triangles in the solution of the electric field integral equation," *IEEE Trans. Antennas Propagat.*, vol. 47, n. 2, pp. 347-353, Feb. 1999.
- [4] R.D. Graglia, G. Lombardi, D.R. Wilton, and W.A. Johnson, "Modeling edge singularities in the method of moments," *Proceedings of the IEEE AP-S International Symposium and URSI National Radio Science Meeting*, Washington, DC, USA, vol. AP-S, July 2005.